COMETARY SCIENCE

# On the nucleus structure and activity of comet 67P/Churyumov-Gerasimenko

Holger Sierks,[1*] Cesare Barbieri,[2] Philippe L. Lamy,[3] Rafael Rodrigo,[4,5] Detlef Koschny,[6] Hans Rickman,[7,8] Horst Uwe Keller,[9,10] Jessica Agarwal,[1] Michael F. A'Hearn,[1,11,12] Francesco Angrilli,[13] Anne-Therese Auger,[14] M. Antonella Barucci,[15] Jean-Loup Bertaux,[16] Ivano Bertini,[17] Sebastien Besse,[6] Dennis Bodewits,[11] Claire Capanna,[14] Gabriele Cremonese,[18] Vania Da Deppo,[19] Björn Davidsson,[7] Stefano Debei,[13] Mariolino De Cecco,[20] Francesca Ferri,[17] Sonia Fornasier,[15] Marco Fulle,[21] Robert Gaskell,[22] Lorenza Giacomini,[17] Olivier Groussin,[14] Pablo Gutierrez-Marques,[1] Pedro J. Gutiérrez,[23] Carsten Güttler,[1] Nick Hoekzema,[1] Stubbe F. Hviid,[1,10] Wing-Huen Ip,[24,25] Laurent Jorda,[14] Jörg Knollenberg,[10] Gabor Kovacs,[1] J. Rainer Kramm,[1] Ekkehard Kührt,[10] Michael Küppers,[26] Fiorangela La Forgia,[2] Luisa M. Lara,[23] Monica Lazzarin,[2] Cédric Leyrat,[15] Josè J. Lopez Moreno,[23] Sara Magrin,[2] Simone Marchi,[27] Francesco Marzari,[2] Matteo Massironi,[17,28] Harald Michalik,[29] Richard Moissl,[26] Stefano Mottola,[10] Giampiero Naletto,[17,19,30] Nilda Oklay,[1] Maurizio Pajola,[17] Marco Pertile,[13,17] Frank Preusker,[10] Lola Sabau,[31] Frank Scholten,[10] Colin Snodgrass,[1]† Nicolas Thomas,[32,33] Cecilia Tubiana,[1] Jean-Baptiste Vincent,[1] Klaus-Peter Wenzel,[6] Mirco Zaccariotto,[13,17] Martin Pätzold[34]

**Images from the OSIRIS scientific imaging system onboard Rosetta show that the nucleus of 67P/Churyumov-Gerasimenko consists of two lobes connected by a short neck. The nucleus has a bulk density less than half that of water. Activity at a distance from the Sun of >3 astronomical units is predominantly from the neck, where jets have been seen consistently. The nucleus rotates about the principal axis of momentum. The surface morphology suggests that the removal of larger volumes of material, possibly via explosive release of subsurface pressure or via creation of overhangs by sublimation, may be a major mass loss process. The shape raises the question of whether the two lobes represent a contact binary formed 4.5 billion years ago, or a single body where a gap has evolved via mass loss.**

Since 23 March 2014 at a distance of 5 million km, the Optical, Spectroscopic, and Infrared Remote Imaging System [OSIRIS (*1*)] onboard the Rosetta spacecraft has been regularly imaging the nucleus of comet 67P/Churyumov-Gerasimenko (hereafter 67P) and its dust and gas environment in 25 broad- and narrow-band filters covering the wavelength range 240 to 1000 nm through its narrow- and wide-angle cameras, NAC and WAC [details in supplementary text 1 (SM1)]. The data thus far have provided a view of this comet at variance with our earlier knowledge [reviewed in (*2*)].

## Bulk properties and rotation

The rotation period determined from early, unresolved observations was 12.4043 ± 0.0007 hours (*3*), implying a decrease of the spin period by 0.36 hours during (or since) the 2009 perihelion passage, consistent with the range predicted for the 2015 perihelion passage (*4*).

The nucleus was first resolved in the NAC (>1 pixel) on 16 June 2014, at a distance of 192,000 km, and the resolution has improved to 0.15 m/pixel at a distance of 10 km at the time of writing.

Starting in August 2014, when the comet was well enough resolved, a more accurate approach based on tracking stereo landmarks was used to determine the direction of the spin axis. Three different algorithms led to a prograde spin axis at RA = 69.3° ± 0.1°, Dec = 64.1° ± 0.1°, in good agreement with (*3*). We found no obvious evidence for complex rotation, and the current result constrains any motion of the spin axis to <0.3° over ~55 days. The lack of measurable change over such a short time scale is not yet a useful constraint on torques.

Early shape models of the nucleus were constructed from images acquired through September 2014, with a best resolution of 0.8 m/pixel. Stereo-photogrammetry [(*5*) and references therein] and stereophotoclinometry (*6*) yielded high-resolution (5 to 10 m) shape models (Fig. 1). The shape has a very pronounced bilobe appearance, reminiscent of comets 8P/Tuttle (*7*) and 103P/Hartley 2 (*8*). The lobes in these two comets are aligned roughly along their longest axes, whereas in 67P the alignment appears more nearly perpendicular to the axes of the individual lobes, and the axis of rotation is closer to parallel to the long axes of the lobes. From the three-dimensional shape models, the larger lobe (the body) has a size of about 4.1 × 3.3 × 1.8 km, and the smaller lobe (the head) is 2.6 × 2.3 × 1.8 km; they are connected by a short "neck." The total volume, estimated by adding limb scans from the microwave instrument onboard Rosetta (MIRO) to fill in the unmapped portions around the southern (negative) rotational pole, is 21.4 ± 2.0 $km^3$.

The current shape model is not complete because the obliquity of the comet's rotational axis (52°) currently puts the southern (negative) pole in permanent shadow (it will have continuous sunlight at perihelion, 13 August 2015; equinox in May 2015). The volume of the model yields a mean density of 470 ± 45 $kg/m^3$ when combined with the mass, $1.0 \times 10^{13}$ kg, determined by the Radio Science Investigation (RSI) instrument (*9*). Although the principal axes of the shape model are still uncertain because of the unmapped portion of the nucleus, they are consistent with simple rotation about the axis of maximum moment of inertia, assuming homogeneous density. The determined density implies high porosity, in the range of 70 to 80% depending on the adopted dust-to-ice mass ratio, or equivalently the bulk density for a solid mixture of ice and dust, which we assume to be 1500 to 2000 $kg/m^3$.

[1]Max-Planck-Institut für Sonnensystemforschung, 37077 Göttingen, Germany. [2]Department of Physics and Astronomy, University of Padova, 35122 Padova, Italy. [3]Laboratoire d'Astrophysique de Marseille, UMR 7326, CNRS & Aix Marseille Université, 13388 Marseille Cedex 13, France. [4]Centro de Astrobiologia, CSIC-INTA, 28850 Madrid, Spain. [5]International Space Science Institute, 3012 Bern, Switzerland. [6]Scientific Support Office, European Space Research and Technology Centre/ESA, 2201 AZ Noordwijk ZH, Netherlands. [7]Department of Physics and Astronomy, Uppsala University, 75120 Uppsala, Sweden. [8]PAS Space Research Center, 00716 Warszawa, Poland. [9]Institut für Geophysik und extraterrestrische Physik, Technische Universität Braunschweig, 38106 Braunschweig, Germany. [10]Deutsches Zentrum für Luft- und Raumfahrt, Institut für Planetenforschung, 12489 Berlin, Germany. [11]Department of Astronomy, University of Maryland, College Park, MD 20742, USA. [12]Akademie der Wissenschaften zu Göttingen, 37077 Göttingen, Germany. [13]Department of Industrial Engineering, University of Padova, 35131 Padova, Italy. [14]Aix Marseille Université, CNRS, Laboratoire d'Astrophysique de Marseille, UMR 7326, 13388 Marseille, France. [15]LESIA–Observatoire de Paris, CNRS, Université Pierre et Marie Curie, Université Paris Diderot, 92195 Meudon, France. [16]LATMOS, CNRS/UVSQ/IPSL, 78280 Guyancourt, France. [17]Centro di Ateneo di Studi ed Attività Spaziali "Giuseppe Colombo" (CISAS), University of Padova, 35131 Padova, Italy. [18]INAF, Osservatorio Astronomico di Padova, 35122 Padova, Italy. [19]CNR-IFN UOS Padova LUXOR, 35131 Padova, Italy. [20]University of Trento, 38100 Trento, Italy. [21]INAF - Osservatorio Astronomico di Trieste, 34014 Trieste, Italy. [22]Planetary Science Institute, Tucson, AZ 85719, USA. [23]Instituto de Astrofisica de Andalucia (CSIC), c/ Glorieta de la AstronomÌa s/n, 18008 Granada, Spain. [24]Graduate Institute of Astronomy, National Central University, Chung-Li 32054, Taiwan. [25]Space Science Institute, Macau University of Science and Technology, Macao, China. [26]Operations Department, European Space Astronomy Centre/ESA, 28691 Villanueva de la Canada, Madrid, Spain. [27]Solar System Exploration Research, Virtual Institute, Southwest Research Institute, Boulder, CO 80302, USA. [28]Dipartimento di Geoscienze, University of Padova, 35131 Padova, Italy. [29]Institut für Datentechnik und Kommunikationsnetze der TU Braunschweig, 38106 Braunschweig, Germany. [30]Department of Information Engineering, University of Padova, 35131 Padova, Italy. [31]Instituto Nacional de Tecnica Aeroespacial, 28850 Torrejon de Ardoz, Madrid, Spain. [32]Physikalisches Institut, University of Bern, 3012 Bern, Switzerland. [33]Center for Space and Habitability, University of Bern, 3012 Bern, Switzerland. [34]Rheinisches Institut für Umweltforschung, Abteilung Planetenforschung, Universität zu Köln, 50931 Köln, Germany.
***Corresponding author. E-mail: sierks@mps.mpg.de** †Present address: Planetary and Space Sciences, Department of Physical Sciences, Open University, Milton Keynes MK7 6AA, UK.

This low density confirms previous results for other comets based on indirect and less precise determinations, mostly from modeling nongravitational accelerations but also including the breakup of comet D/Shoemaker-Levy 9 (1993 F2), the fallback under gravity of the Deep Impact ejecta, and the lower limit on porosity (75%) of the upper 1 to 10 m from the faintness of the impact flash of Deep Impact [e.g., (10–13); review in (14)]. In fact, the mass is almost the same as deduced from the nongravitational acceleration but with larger uncertainty (10). Thus, we now constrain the porosity of a cometary nucleus even more tightly. The agreement between the axis of rotation and the axis of maximum moment of inertia reinforces the concept of weakly bonded icy dust aggregates, with porosity at small scales relative to the size of the nucleus (rather than large voids). This conclusion is further strengthened by the very low strength (10 Pa) deduced by (15).

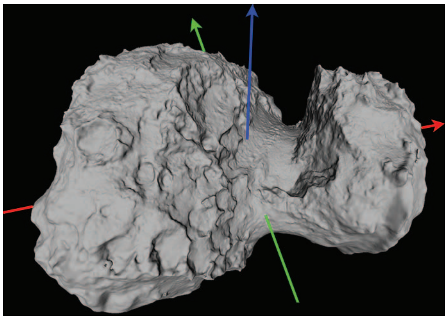

**Fig. 1. Stereophotogrammetric shape models of comet 67P.** The blue arrow indicates 67P's rotation axis *z*; the red and green arrows display its equatorial *x* and *y* axes (*x* according to the current zero-longitude definition). If the nucleus is homogeneous in density, the axis of minimum moment of inertia is consistent with being in the equatorial plane.

We have calculated the gravitational and centrifugal forces on the same shape model. As shown (Fig. 2), the gravitational potential varies by less than a factor of 2. The centrifugal force varies from negligible to one-third of the gravitational force. However, the surface slope relative to local gravity varies markedly, with many areas exceeding 45° (Fig. 2). Escape velocity at the surface is poorly defined because nuclear rotation causes the gravitational acceleration to vary by a large factor in the time taken to move 1 nuclear radius. For a sphere with the same density and volume (radius = 1.72 km), the escape velocity would be 0.9 m/s, roughly three times the velocity deduced via the same approximation for comet 103P/Hartley 2 (16).

67P's two main lobes show considerable morphological diversity (15), and the neck is different from both. Geomorphological regions are identified in Fig. 3 [see (15) for more detail] and, following the ancient Egyptian theme of the Rosetta mission, they are named for Egyptian deities. The entire nucleus is dark, yielding a geometric albedo of the entire nucleus of only 5.9 ± 0.2% at 550 nm, similar to that of comet 9P/Tempel 1 (17). Despite the extreme morphological diversity, colorimetry of the nucleus is remarkably uniform, except in the Hapi region on the neck (SM2). Whether this is due to redeposited material on both lobes or implies that both lobes are intrinsically similar is still an open question.

## Activity and its source

OSIRIS has detected the presence of a dust coma since the pronounced outburst between 27 and 30 April 2014, or even earlier (18). We detected resolved features in the coma (SM2) in long WAC exposures with the 610-nm filter (SM1) at the end of July 2014, when the comet was 3.7 AU from the Sun and the spacecraft distance was 3000 km. Most of the activity was unambiguously coming out of the transition region between the small and large lobes of the nucleus, the Hapi region, or very close to it. This was consistent with ground-based observations of coma structures over the last two orbital periods, which implied an active region at high northern (positive) latitude (19). When the spacecraft distance dropped to 100 km (resulting in a resolution of 1.8 m/pixel in NAC, 10 m/pixel in WAC), it was possible to localize the active sources by inversion of the jets. Most of the jets arose from Hapi, at about +60° latitude (Fig. 4), although we found other minor active spots on both lobes of the nucleus (SM3). This major coma feature presents a diurnal variation of intensity due to changing insolation conditions and observational geometry: A planar fan-like jet appears brighter and more focused when viewed edge-on rather than face-on.

To investigate why the activity is dominant above Hapi, we calculated the energy incident on all parts of the nucleus over one rotation on 6 August 2014. According to the model as applied to the shape model of 67P (20), self-heating by thermal reradiation from the head and the body provides extra heating to the region of the neck and at the time of peak jet activity, and parts of Hapi and Hathor receive 10% higher flux than other regions. However, at this point in the orbit, the rotational axis is oriented so that the neck receives slightly less energy over a rotation than do other parts of the nucleus (Fig. 5). This suggests a large compositional (e.g., type of ice) or structural (e.g., depth of ice) difference in Hapi relative to other regions. More detailed models that take sublimation and thermal inertia into account are needed to clarify the situation. Because of the large obliquity of the rotational axis with respect to the orbital plane, it is likely that the currently

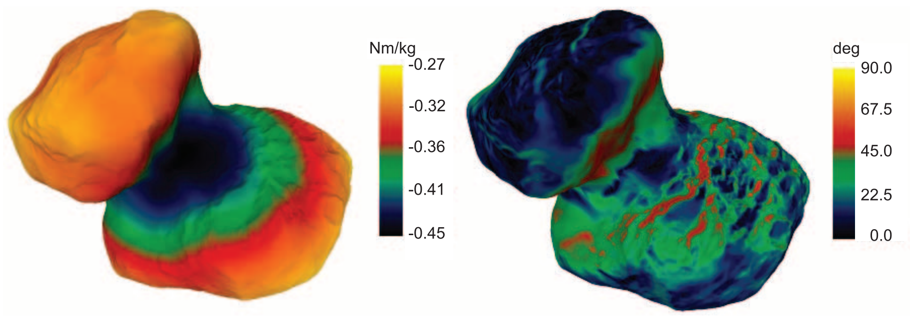


**Fig. 2. Gravitational field.** Left: The effective gravitational potential at the surface, including the centrifugal term due to rotation of the nucleus, is shown looking toward the neck from an intermediate latitude in the northern (positive) hemisphere (between the blue and red arrows in Fig. 1). Right: The slope of the terrain relative to local gravity.

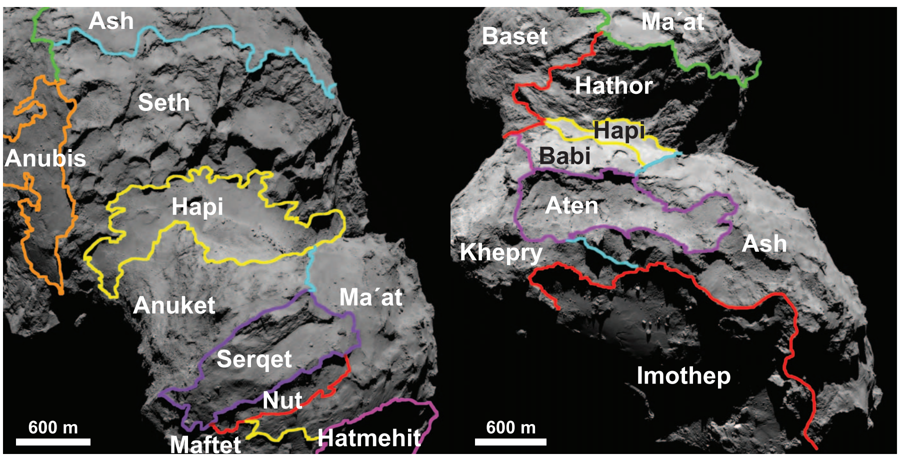


**Fig. 3. Geomorphological map of comet 67P.** Left: Region definition for one face of 67P, showing the Seth region on the body and the smooth Hapi region on the neck. Other regions are defined in more detail by (15). Right: Regional definition looking from the body (foreground) across to the head.

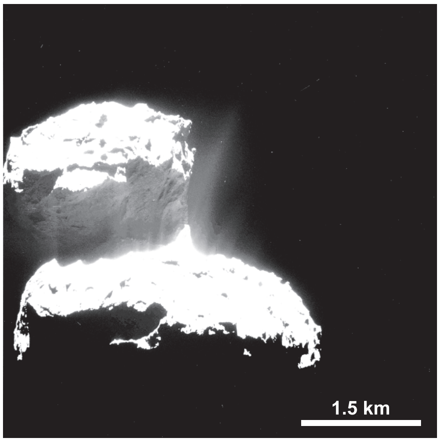


**Fig. 4. Jets.** Jets from the Hapi region as observed on 23 September 2014.

active northern (positive) hemisphere has evolved very differently than has the southern (negative, thus far only partially mapped) hemisphere.

### Nuclear properties and geomorphology

In the Seth region, extending around the neck from one end of Hapi (Fig. 3), we observe a closely packed system of well-defined pits and depressions with remarkably flat floors. The walls of these features show linear structures that are parallel to their floors and extend laterally hundreds of meters, indicating a consolidated structure, but they also exhibit vertical striations. Some of these quasi-circular pits are minor sources of activity (e.g., Fig. 6). They are similarly seen in cliffs and are possibly erosion features related to activity. They range from 50 to 300 m in diameter and 10 to 200 m in depth. We find other pits everywhere on the nucleus. Such pits have been observed on comets 81P/Wild 2 and 9P/Tempel 1, and those were interpreted as activity-related features rather than impact craters because of their flat size distribution (*21*). The pits on the nucleus of 67P share a similar morphology, although the active ones tend to have a depth/diameter ratio close to 1, whereas the inactive pits are much shallower, seemingly filled with fine dust and multiple boulders. It is not clear whether these pits are inactive or whether they will "wake up" when they start receiving more illumination.

The head is characterized by impressive cliffs and sets of aligned linear structures >500 m in length exposed at the cliff facing the neck (Hathor) (Fig. 7). This cliff is opposite Seth, which has a different character. Fracturing is seen over the nucleus at all scales, except where the nucleus appears to be covered with smooth deposits. Small-scale fracturing appears more scattered than the larger-scale linear structures. Thermal shock may be a plausible mechanism given the very large variation in temperatures seen by cometary nuclei; the near-surface region of 67P undergoes fluctuations of up to 150 K each orbital period, much larger than those invoked to explain linear structures on Eros (*22*). The surface morphology strongly suggests that the loss of larger volumes of material, possibly via the explosive release of subsurface gas pressure or creation of overhangs by sublimation, may be a major mass loss process for the nucleus.

We observe irregular quasi-linear features at the Anuket-Hathor interface, which we infer to be cracks in the surface of the neck (Fig. 7). These cracks include ones that are roughly parallel to the neck. We note that within the Hapi region there is also an open crack, which is similarly aligned (Fig. 7) and extends well into Anuket. The fact that they are more or less parallel and across the neck suggests that they may be related to each other and to large-scale phenomena on the nucleus, such as flexure between the head and the body.

There are also clusters of small, bright spots (0.5 to 1 m), which might be ice-rich, and there are both groups and isolated examples of much larger clumps (up to 30 m).

Finally, we have found in several places on the nucleus, particularly on very steep slopes, a feature that we colloquially term "goosebumps" (Fig. 8). The bumps themselves exhibit a characteristic scale of about 3 m. Although we do not yet have an interpretation of these features, the fact that a single characteristic scale is present may be an important clue to formation processes, as many of the possible processes have characteristic scales.

### The origin of 67P/Churyumov-Gerasimenko

One key question about the origin of 67P is whether its nucleus is a primordial planetesimal or was formed from a much larger planetesimal. To address this, we must ask how the present 67P nucleus evolved since it formed eons ago.

Two modes of formation of original planetesimals in the outer parts of the solar system

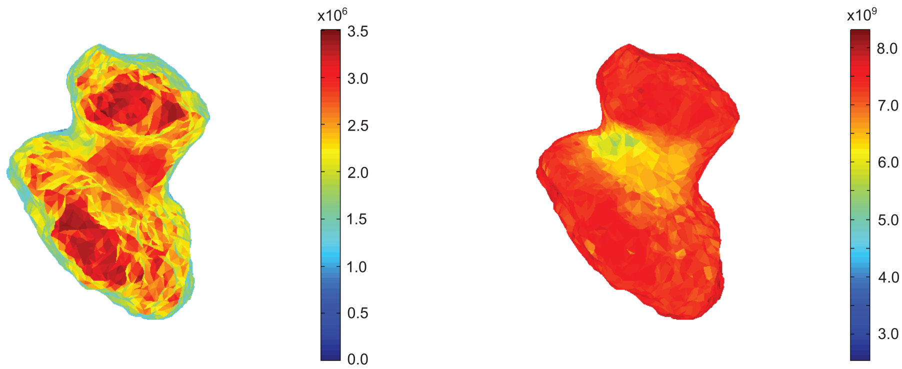


**Fig. 5. Map of energy input.** Left: A map looking at the northern (right-hand rule, positive) pole of 67P showing the total energy received from the Sun per rotation on 6 August 2014. The energy received includes thermal illumination by the surfaces of the comet itself. The base of the neck (Hapi) receives ~15% less energy than the most illuminated region, $3.5 \times 10^6$ J m$^{-2}$ (per rotation). If self-heating were not included, the base of the neck would receive ~30% less total energy. Right: Similar to the left panel but showing total energy received over an entire orbital period in J m$^{-2}$ (per orbit). This heating varies by only ~50% over the entire surface. Although not shown here, the opposite hemisphere receives essentially the same energy, but at a higher rate over a shorter time.

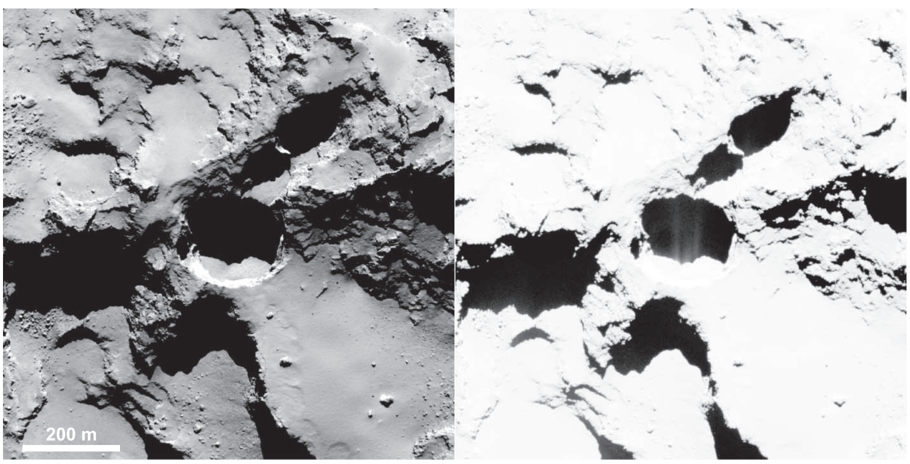


**Fig. 6. Active pits detected in Seth region.** NAC image acquired on 28 August 2014. Distance to the comet, 60 km; resolution, 1 m/pixel. Enhancing the contrast (right panel) shows fine structures in the shadow of the pit, interpreted as fine jets arising from the pit.

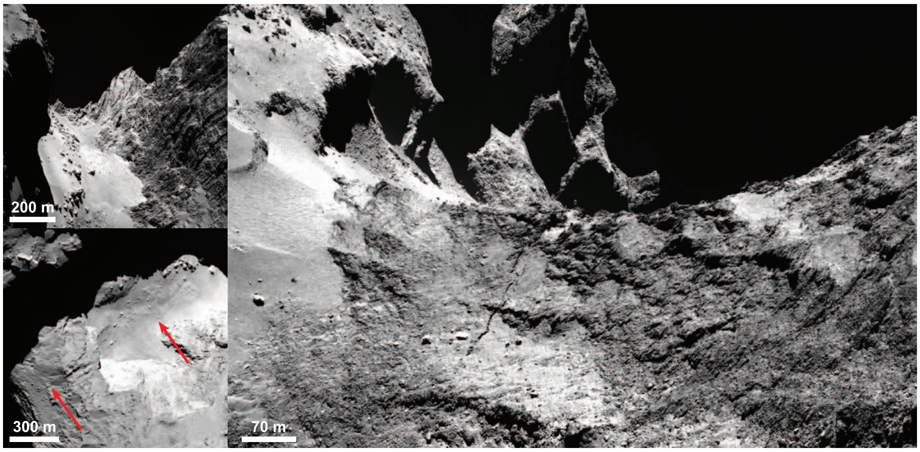


**Fig. 7. Nucleus close-ups.** Top left: The Hathor cliff face is to the right in this view. The aligned linear structures can be clearly seen. The smooth Hapi region is seen at the base of the Hathor cliff. Boulders are prevalent along the long axis of the Hapi region. Bottom left and right: Crack in the Hapi region. The left panel shows the crack (indicated by red arrows) extending across Hapi and beyond. The right panel shows the crack where it has left Hapi and is extending into Anuket, with Seth at the uppermost left and Hapi in the lower left.

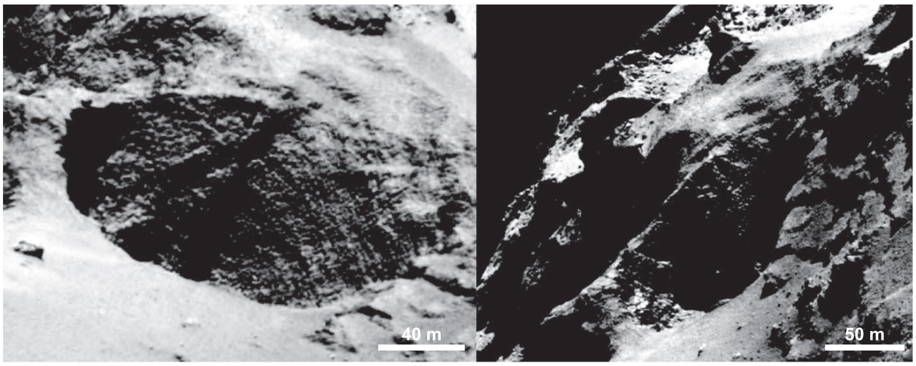


**Fig. 8. Goosebumps.** Characteristic scale of all the bumps is ~3 m, extending over >100 m. This example is in the active pit in the Seth region.

are well developed: hierarchical accretion (*23*) and clumping of "pebbles" due to gas-dust instabilities. In both cases, accretional velocities were likely very low. The pebble swarms caused by the dynamical instabilities may form objects as large as $10^2$ to $10^3$ km or as small as the 67P nucleus (*24*), although the goosebumps mentioned above suggest that a smaller scale could be important. Small objects could also form later as individual or reaccreted fragments produced by collisions involving large transneptunian objects (*25*), but these may be different from the small, original planetesimals, having experienced the radioactive heating of their large parent bodies and the impacts whereby they were ejected.

The amount of previous erosion of the 67P nucleus depends on the dynamical age of the comet—that is, the number of orbits it has performed as a member of the Jupiter family after its capture from the transneptunian reservoir (SM4). Unfortunately, this number is unknown and will remain so, because in the presence of frequent close encounters with Jupiter inducing strong orbital perturbations, the dynamical evolution of Jupiter family comets is strongly chaotic. Thus, the orbital history of 67P can be traced back past a close encounter in 1959 (minimum distance from Jupiter = 0.05 AU) [(*26*, *27*); see (*28*) and SM4 for sample calculations] but not much further.

A key question that Rosetta will address during the escort phase of the mission is whether the two lobes of the nucleus are separate cometesimals or whether the neck region has been carved out by erosion. If the head and the body turn out to be very different in composition or internal structure, this would argue for the idea that they are original cometesimals. If they are similar in composition and structure, the conclusion is less clear-cut. The two lobes, head and body, could still be separate cometesimals that formed at essentially the same heliocentric distance and time. Whether the neck could also be the result of erosion of a more convex body over many orbital revolutions remains to be clarified. Our study of energy input described above shows that this is not enough focused to the neck (SM5), but the question of whether fragmentation can still be sufficiently localized to cause the carving remains unresolved.

Some key features relevant to the formation are the high porosity implied by the bulk density (SM6), the pristine composition evidenced by the large abundance of CO (*29*), and the possible evidence of fracturing in the head and neck region (SM7). The primordial accretion model seems consistent with all observations. The scenario of colliding large bodies seems to require more special circumstances, tending to make it less attractive but still viable.

## REFERENCES AND NOTES

1. H. U. Keller *et al*., OSIRIS—The scientific camera system onboard Rosetta. *Space Sci. Rev.* **128**, 433–506 (2007). doi: 10.1007/s11214-006-9128-4
2. P. L. Lamy *et al*., A portrait of the nucleus of comet 67P/Churyumov-Gerasimenko. *Space Sci. Rev.* **128**, 23–66 (2007). doi: 10.1007/s11214-007-9146-x
3. S. Mottola *et al*., The rotation state of 67P/Churyumov-Gerasimenko from approach observations with the OSIRIS cameras on Rosetta. *Astron. Astrophys*. **569**, id.L2 (2014). doi: 10.1051/0004-6361/201424590
4. P. J. Gutiérrez, L. Jorda, N. H. Samarasinha, P. Lamy, Outgassing-induced effects in the rotational state of comet 67P/Churyumov-Gerasimenko during the Rosetta mission. *Planet. Space Sci.* **53**, 1135–1145 (2005). doi: 10.1016/j.pss.2004.12.012
5. F. Preusker *et al*., The northern hemisphere of asteroid (21) Lutetia—topography and orthoimages from Rosetta OSIRIS NAC image data. *Planet. Space Sci.* **66**, 54–63 (2012). doi: 10.1016/j.pss.2012.01.008
6. R. W. Gaskell *et al*., Characterizing and navigating small bodies with imaging data. *Meteorit. Planet. Sci.* **43**, 1049–1061 (2008). doi: 10.1111/j.1945-5100.2008.tb00692.x
7. J. K. Harmon, M. C. Nolan, J. D. Giorgini, E. S. Howell, Radar observations of 8P/Tuttle: A contact-binary comet. *Icarus* **207**, 499–502 (2010). doi: 10.1016/j.icarus.2009.12.026
8. P. C. Thomas *et al*., Shape, density, and geology of the nucleus of Comet 103P/Hartley 2. *Icarus* **222**, 550–558 (2013). doi: 10.1016/j.icarus.2012.05.034
9. ESA, "Determining the mass of comet 67P/C-G" (blog entry); http://blogs.esa.int/rosetta/2014/08/21/determining-the-mass-of-comet-67pc-g/.
10. B. J. R. Davidsson, P. J. Gutiérrez, Nucleus properties of comet 67P/Churyumov-Gerasimenko estimated from non-gravitational force modeling. *Icarus* **176**, 453–477 (2005). doi: 10.1016/j.icarus.2005.02.006
11. E. Asphaug, W. Benz, Density of comet Shoemaker-Levy 9 deduced by modelling breakup of the parent 'rubble pile'. *Nature* **370**, 120–124 (2004). doi: 10.1038/370120a0
12. C. M. Ernst, P. H. Schultz, Evolution of the Deep Impact flash: Implications for the nucleus surface based on laboratory experiments. *Icarus* **190**, 334–344 (2007). doi: 10.1016/j.icarus.2007.03.030
13. J. E. Richardson, H. J. Melosh, C. M. Lisse, B. Carcich, A ballistics analysis of the deep impact ejecta plume: Determining comet Tempel 1's gravity, mass, and density. *Icarus* **190**, 357–390 (2007). doi: 10.1016/j.icarus.2007.08.001
14. M. F. A'Hearn, Comets as building blocks. *Annu. Rev. Astron. Astrophys.* **49**, 281–299 (2011). doi: 10.1146/annurev-astro-081710-102506
15. N. Thomas *et al*., The morphological diversity of comet 67P/Churyumov-Gerasimenko. *Science* **347**, aaa0440 (2015).
16. B. Hermalyn *et al*., The detection, localization, and dynamics of large icy particles surrounding comet 103P/Hartley 2. *Icarus* **222**, 625–633 (2013). doi: 10.1016/j.icarus.2012.09.030
17. J.-Y. Li *et al*., Deep Impact photometry of comet 9P/Tempel 1. *Icarus* **191**, 161–175 (2007). doi: 10.1016/j.icarus.2006.09.027
18. C. Tubiana *et al*., 67P/Churyumov-Gerasimenko: Activity between March and June 2014 as observed from Rosetta/OSIRIS. *Astron. Astrophys*. **573**, id.A62 (2015). doi: 10.1051/0004-6361/201424735
19. J.-B. Vincent, L. M. Lara, G. P. Tozzi, Z.-Y. Lin, H. Sierks, Spin and activity of comet 67P/Churyumov-Gerasimenko. *Astron. Astrophys.* **549**, id.A121 (2013). doi: 10.1051/0004-6361/201219350
20. B. J. R. Davidsson, H. Rickman, Surface roughness and three-dimensional heat conduction in thermophysical models. *Icarus* **243**, 58–77 (2014). doi: 10.1016/j.icarus.2014.08.039
21. M. J. S. Belton, P. D. Feldman, M. F. A'Hearn, B. Carcich, Cometary cryo-volcanism: Source regions and a model for the UT 2005 June 14 and other mini-outbursts on Comet 9P/Tempel 1. *Icarus* **198**, 189–207 (2008). doi: 10.1016/j.icarus.2008.07.009

22. D. A. J. Dombard, A. M. Freed, Thermally induced lineations on the asteroid Eros: Evidence of orbit transfer. *Geophys. Res. Lett.* **29**, 65-1–65-4 (2002). doi: 10.1029/2002GL015181
23. S. J. Weidenschilling, From icy grains to comets. In *Comets II*, M. C. Festou, H. U. Keller, H. A. Weaver, Eds. (University of Arizona Press, Tucson, 2004), pp. 97–104.
24. K. W. Janson, A. Johansen, Formation of pebble-pile planetesimals. *Astron. Astrophys.* **570**, A47 (2014). doi: 10.1051/0004-6361/201424369
25. D. R. Davis, P. Farinella, Collisional evolution of Edgeworth-Kuiper belt objects. *Icarus* **125**, 50–60 (1997). doi: 10.1006/icar.1996.5595
26. A. Carusi, L. Kresák, E. Perozzi, G. B. Valsecchi, *Long-Term Evolution of Short-Period Comets* (Adam-Hilger, Bristol, UK, 1985).
27. N. A. Belyaev, L. Kresak, E. M. Pittich, A. N. Pushkarev, *Catalogue of Short-Period Comets* (Astronomical Institute of the Slovak Academy of Sciences, Bratislava, 1986).
28. O. Groussin, G. Hahn, P. Lamy, R. Gonczi, G. B. Valsecchi, The long-term evolution and initial size of comets 46P/Wirtanen and 67P/Churyumov-Gerasimenko. *Mon. Not. R. Astron. Soc.* **376**, 1399–1406 (2007). doi: 10.1111/j.1365-2966.2007.11553.x
29. M. Haessig *et al*., The variability and heterogeneity in the coma of 67P/Churyumov-Gerasimenko. *Science* **347**, aaa0276 (2015).

## ACKNOWLEDGMENTS

In memory of our colleague and co-investigator, Michel Festou. We thank our retired co-investigators M. E. Bailey, P. Barthol, J. A. Burns, W. Curdt, F. Gliem, A. Llebaria, and J. P. Sivan for their contribution to the success of OSIRIS, as well as the team of optical, electrical, mechanical, thermal, and software engineers that turned the instrument into reality and supported it throughout in flight operations. OSIRIS was built by a consortium led by the Max-Planck-Institut für Sonnensystemforschung, Göttingen, Germany, in collaboration with CISAS, University of Padova, Italy, the Laboratoire d'Astrophysique de Marseille, France, the Instituto de Astrofísica de Andalucia, CSIC, Granada, Spain, the Scientific Support Office of the European Space Agency, Noordwijk, Netherlands, the Instituto Nacional de Técnica Aeroespacial, Madrid, Spain, the Universidad Politéchnica de Madrid, Spain, the Department of Physics and Astronomy of Uppsala University, Sweden, and the Institut für Datentechnik und Kommunikationsnetze der Technischen Universität Braunschweig, Germany. The support of the national funding agencies of Germany (DLR), France (CNES), Italy (ASI), Spain (MEC), Sweden (SNSB), and the ESA Technical Directorate is gratefully acknowledged. We acknowledge the support of the local institutes that realized the instrument. Also supported by NASA JPL contract 1267923 to the University of Maryland (M.F.A'H.), grant NSC 101-2111-M-008-016 from the Ministry of Science and Technology, Taiwan (W.H.I.), grant 2011/01/B/ST9/05442 from the Polish National Science Center and grant 74/10:2 of the Swedish National Space Board (H.R.), and travel grants from the Swiss National Science Foundation (N.T.). All data presented in this paper will be delivered to ESA's Planetary Science Archive and NASA's Planetary Data System in accordance with the schedule established by the Rosetta project and will be available on request prior to that archiving. We thank the Rosetta Science Ground Segment at ESAC, the Rosetta Mission Operations Centre at ESOC, and the Rosetta Project at ESTEC for their outstanding work enabling the science return of the Rosetta Mission. The OSIRIS team thanks the MIRO team and its principal investigator, S. Gulkis, for providing prepublication data and helpful discussion regarding use of their limb scans to determine the shape.

## SUPPLEMENTARY MATERIALS

www.sciencemag.org/content/347/6220/aaa1044/suppl/DC1
Supplementary Text
Figs. S1 to S7
Table S1
References (*30*–*42*)

17 October 2014; accepted 30 December 2014
10.1126/science.aaa1044